Astronomical and Astrophysical Transactions (*AApTr*), 2023, Vol. 34, Issue 1, pp. 65–84,
ISSN 1055-6796, Photocopying permitted by license only, ©Cambridge Scientific Publishers

Physical bases of the short-term forecast of earthquakes

S.A. Pulinets*

[1] *Space Research Institute (IKI), Russian Academy of Sciences, Profsoyuznaya Str. 84/32, Moscow, 117997 Russia*

Received 13 October, 2023

A concept of short-term forecasting of destructive earthquakes, based on regular monitoring of atmospheric and ionospheric parameters, is presented. Physical mechanisms for the generation of specific variations in the atmosphere, ionosphere and magnetosphere of the earth have been revealed, allowing them to be unambiguously identified as short-term precursors of earthquakes. It has been shown that indicators of earthquake preparation are a consequence of ionization of the atmospheric boundary layer and are similar to other processes associated with ionization, such as the clouds formation under the galactic cosmic ray's fluxes impact or the generation of thermal anomalies during accidents at nuclear power plants or other emissions of radioactive substances into the atmosphere. The effects of earthquake preparation are part of the general process of the geosphere's interaction.

Keywords: Earthquake precursors, radon, GPS TEC, relative air humidity

1 Introduction

The problem of short-term earthquake forecasting has a rather complicated history and has not yet been solved (Pulinets and Ouzounov, 2018). The main reason is that the physical mechanism of seismogenesis has not been described in seismology to date. Therefore, the problem of prediction in seismology is solved based on the concept of self-organized criticality using statistical methods (Main, 1996). However, the physical approach to earthquake prediction was practiced in seismology 50 years ago (Scholz et al., 1973). Unfortunately, harsh and unfounded criticism of this approach led to the virtual cessation of monitoring of physical precursors, as described in (Scholz et al., 1973), and priority was given to statistical approaches to earthquake forecasting (Geller et al., 1997). At the same time, measurements on artificial Earth satellites regularly demonstrated the appearance of unusual variations in electron concentration, the occurrence of electromagnetic radiation in the VLF range,

*Email: pulse@cosmos.ru

and variations in atmospheric parameters over areas where strong earthquakes are preparing (Larkina et al., 1983; Akhmamedov, 1993; Pulinets, 1998). Systematic observations of similar phenomena in the ionosphere were organized using ground-based and satellite methods, as a result of which it was possible to formulate the main morphological features of ionospheric earthquake precursors (Pulinets et al., 2003). It was the morphology of ionospheric variations before earthquakes that led to the conclusion that the source of these variations could be the electric field at the Earth's surface, and not acoustic-gravity waves, as stated in earlier publications (Pulinets et al., 1998; 2000). The problem remained of what and how the anomalous electric field on the Earth's surface is generated. Our attention was drawn to radon as a source of ions in the atmosphere, formed due to the ionization of gas components of the atmosphere and the possibility of their separation in the natural electric field (Boyarchuk et al., 1997; Pulinets, 2009) of the Global Electric Circuit (GEC) (Mareev, 2010). The experience of calculations used in assessing atmospheric effects during radioactive contamination of the atmosphere (Boyarchuk et al. 2000) was used, taking into account the kinetics of elementary ions in the atmosphere under the influence of ionizing radiation (Boyarchuk, 1997).

The result of the consideration of kinetics was the formation of complex compounds and their hydration, which releases latent heat – a possible source of atmospheric/thermal effects in the atmosphere (Pulinets et al., 2006). When starting to

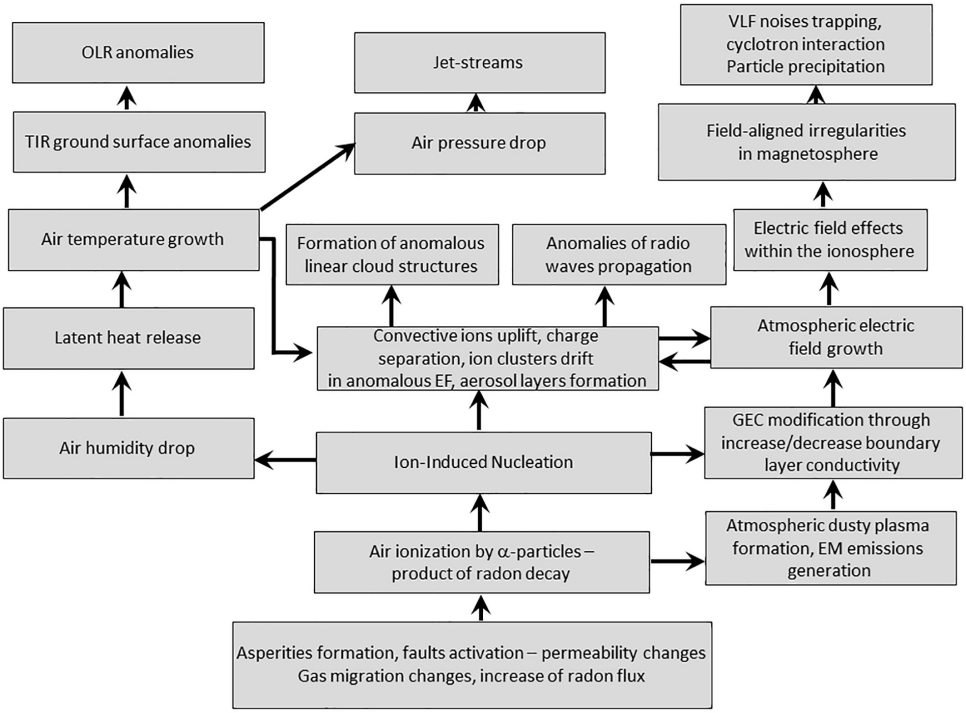


Figure 1 Schematic representation of a complex model of Lithosphere–Atmosphere–Ionosphere coupling (LAIC).

develop the physical mechanism of thermal effects in the atmosphere during the period leading up to earthquakes, we already had information about the presence of such effects based on ground-based measurements in Central Asia (Mil'kis, 1996). As a result, two main directions of research were determined: atmospheric and ionospheric effects formed several days before earthquakes in the area of their preparation and the general concept of Lithosphere–Atmosphere–Ionosphere coupling (Pulinets and Ouzounov, 2011). Its detailed discussion will be one of the main topics of this article. The process of development of thermal and ionospheric pre-earthquake effects includes many other interactions and features, and it is not possible to describe all of them but they are at least indicated in the schematic presentation of the model shown in Fig. 1, and their description is provided in (Pulinets et al., 2022a).

It is obvious that knowledge of the physics of these processes is not yet sufficient to predict earthquakes. It is necessary to establish the statistical reliability of phenomena that claim to be precursors, the possibility of their identification in conditions of high variability of both the atmosphere and the ionosphere, as well as their operational monitoring in real time. These problems will form the basis of the second part of this publication.

In conclusion of this introduction, I would like to note one more important thing. In most publications (including ours), phenomena recorded in the atmosphere and ionosphere before earthquakes are called anomalies. This appears to be incorrect. We do not name as anomalies the variations in the ionosphere during geomagnetic disturbances, we do not name earthquakes or hurricanes themselves as anomalies. All of these are regular geophysical phenomena that reflect the real life of our planet. All mountains, seas, rivers, continents were formed as a result of tectonic activity over 4.5 billion years. And the most important thing which we should keep in mind is that this process has not stopped. And now mountain building is underway, as well as the movement of tectonic plates, the consequence of which are earthquakes and the processes that precede them, which we call precursors. Therefore, earthquake precursors are the same variations in the environment as other geophysical phenomena, and it is in this capacity that they should be considered.

2 Main physical processes generating the earthquake precursors and their similarity to other natural phenomena

Atmospheric ionization processes play an important role in the formation and behavior of the environment, starting with the formation of the plasmasphere and ionosphere and ending with the ionization of the surface layers of the atmosphere. In particular, the effects of corpuscular radiation on the atmosphere can be found in the review (Mironova et al., 2015). As an important addition to this publication, mention should be made of the work (Golubenko et al., 2020), which outlines the important role of atmospheric ionization by radon entering the atmosphere from the Earth's crust, including that leading to modification (GEC). It confirms earlier results (Hoppel et al., 1986) that the natural radioactivity of the Earth is the main source of ionization of the atmosphere at altitudes from the Earth's surface up to 1–2 km, where galactic cosmic rays become the main source of ionization. As was shown in (Pulinets and Boyarchuk, 2004), regardless of the source of ionization, the final result of this process

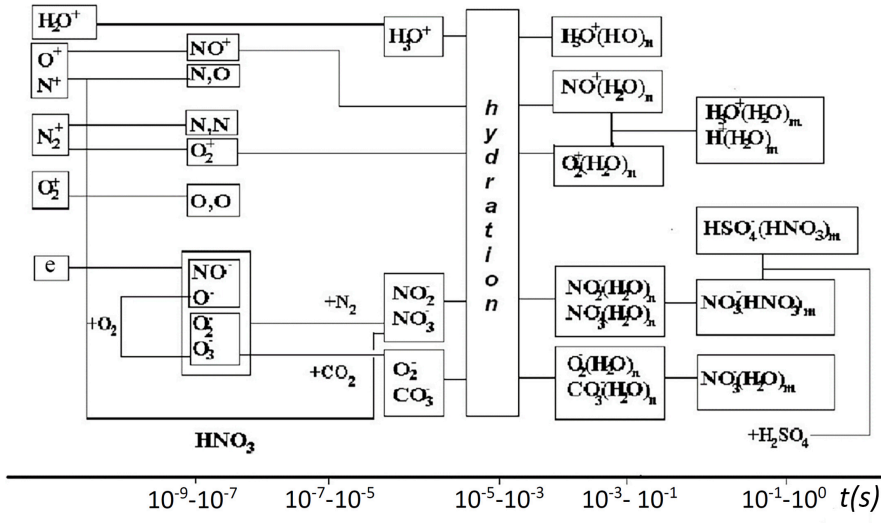


Figure 2 Schematic presentation of the near ground kinetics with basic ion's formation.

is the formation of hydrated cluster ions as a result of plasma-chemical reactions and ion hydration, as shown in Fig. 2. The difference in the final products depends only on the height, and this difference is due to the change in the composition of the troposphere with altitude. At the same time, an important process, which is not always mentioned in publications, is that it is an autocatalytic reaction, which has an explosive nature, and is accompanied by the release latent heat (Timofeev et al., 2003).

We can conclude that the processes of cloud's formation under the action of the galactic cosmic rays (Timofeev et al., 2003) and cluster ion's formation under the action of radon in the near ground layer of the atmosphere (Pulinets and Boyarchuk, 2004) are practically identical. And in both cases the latent heat is released. In the case of galactic cosmic rays they heat the tropopause where the maximum of their relaxation is situated, and radon is heating the boundary layer of the atmosphere (Pulinets et al., 2023). The explosive character of the latent heat release was demonstrated in this paper, and the new integral parameter called "correction of the water vapor chemical potential in atmosphere" (ACP) was proposed which can be expressed by the meteorological parameters: air temperature and relative humidity:

$$\mathrm{ACP} = 5.8 \times 10^{-10}(20T_g + 5463)^2 \ln(100/H), \quad (1)$$

where T_g is near ground air temperature and H is air relative humidity.

This parameter expresses the difference between the bond energy of the water vapor molecule with ion cluster and latent heat constant which is 0.422 eV per one molecule of water in the water drop. Experimentally it was established the maximum values which ACP can reach is nearly 0.1 eV, i.e. about 25% of the latent heat constant.

One more important thing revealed in (Pulinets et al., 2023) is the fact that the ACP parameter can be used as radon proxy, i.e. we can follow the radon activity at

any point in the world (including the ocean surface) using the meteorological parameters air temperature and relative humidity what facilitates the task of geophysical monitoring.

Let us generalize the main peculiarities of the pre-earthquake thermal/meteorological phenomena:

1. Air temperature rise (not coinciding with meteorological forecast)
2. Drop in the air relative humidity (air drying by ions)
3. Drop in the partial water vapor pressure leading to the general (not essential) air pressure drop
4. Vertical air convection increase (possible source of acoustic gravity waves)
5. Formation of so called "earthquake clouds" due to ions induced nucleation (IIN) and rise of the formed nucleus by the vertical convection and anomalous electric field (Morozova et al., 2020)
6. Outgoing longwave infrared radiation (OLR) from the thermal spot (Ouzounov et al., 2006)

All these "side effects" are shown in the schematic presentation of the LAIC model in Fig. 1.

Now let us consider what are the effects in atmospheric electricity and the ionosphere created by ionization which we call the electromagnetic branch of the LAIC model. We again will compare the space weather and pre-earthquake effects starting from the vertical atmospheric electric field (AEF) which is a component of GEC. It is considered that on average the intensity of AEF is of the order of 100 V/m at the ground surface (Hoppel et al., 1986) but during the rush hours in the cities the AEF is growing due to the presence of a large number of aerosols in the air which reduces the vertical air conductivity and leads to an increase of electric potential drop in the boundary layer of atmosphere. If we increase the air conductivity by ionization effect producing a large number of light ions we can increase the air conductivity which will lead to the drop in electric field. Such an effect in AEF is reported during nuclear tests, when the electric field sharply dropped after the nuclear explosion and fast ionization occurred (Holzer, 1972). Returning to Fig. 2 where the large cluster ions formation after the ionization is demonstrated one can expect after the sharp drop of AEF its growth when light ions will transform into heavy cluster ions with extremely low mobility. To check this we consider the effects produced in AEF by a solar proton event and after radon release before two strong earthquakes in Europe and the Kamchatka area which are presented in Fig. 3.

The Space Weather effect (proton event on 17 May 2012) in the left part of Fig. 3 and pre-earthquake effect in the right part are very similar. The only difference is in the intensity of the effect: the AEF variations before earthquakes are much stronger than during the solar proton event.

The next step is even more interesting. Mühleisen (1977) presented the results of more than 15 years radiosonde measurements of the electric field in atmosphere and created the averaged graph showing that during AEF increase the ionospheric potential, which is also is a parameter of GEC, is also increasing. In such a way we get a link to connect the variations of AEF with the ionosphere variations which is the way to the consideration of the ionospheric precursor. In general, if we are to consider radon as the earthquake precursor we should observe first the negative deviation of

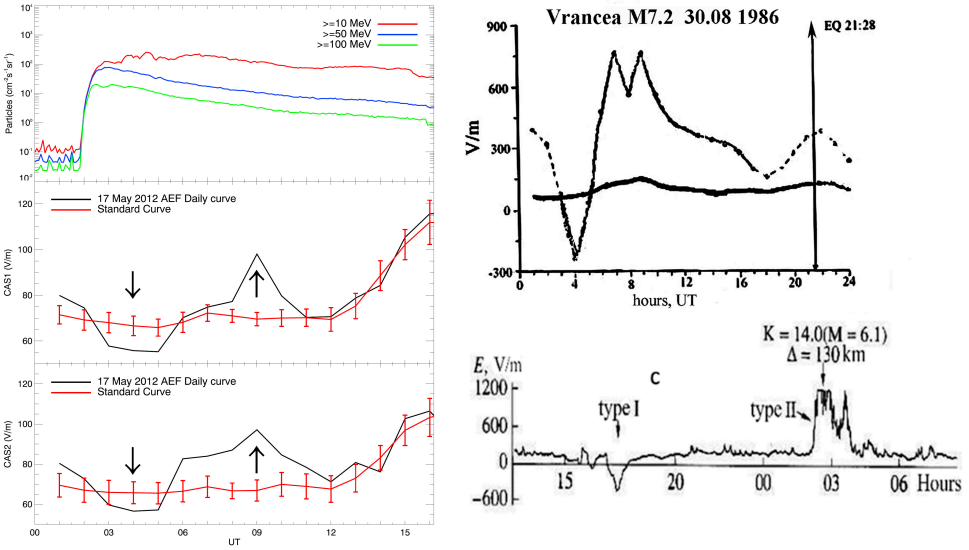


Figure 3 a) From top to bottom: solar proton event on 12 May 2012 in three energy bands, atmospheric electric field (AEF) at two locations and Andes area (Tacza et al., 2018); b) AEF before Vrancea M7.2 earthquake (Nikiforova and Michnovski, 1995); c) AEF before Kamchatka M6.1 earthquake (Vershinin et al., 1999).

the electron concentration in the ionosphere, and then (after ion clusters growth) the positive deviations.

In Fig. 4 the deviations of GPS TEC around the time of M6.1 earthquake in Greece in January 2014 are shown where the TEC deviations from 15-days average are expressed by color. Vertical axis shows the local time, and horizontal axis shows the days of the year. The red triangle on top of the figure shows the moment of earthquake.

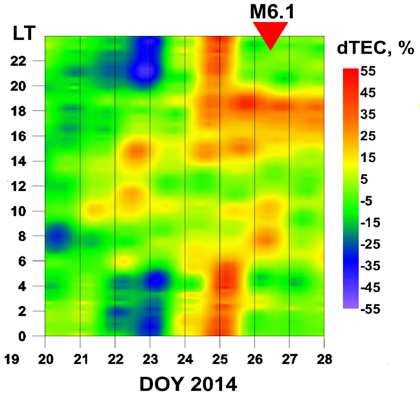


Figure 4 Deviation of the GPS TEC (color coded) around the time of M6.1 earthquake in Greece on 26 January 2014.

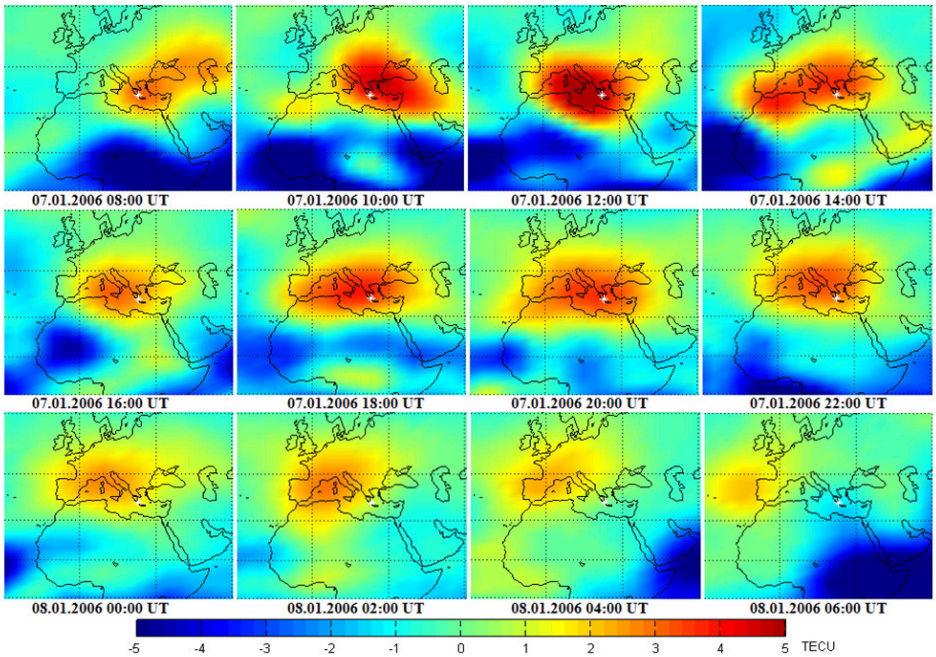


Figure 5 The positive anomalies in the ionosphere one day before an M=6.7 earthquake in Greece on 8 January 2006. Earthquake epicenter is marked by the white cross.

There are different approaches to estimate the pre-earthquake ionospheric disturbances (PEID) from the point of view of initial disturbance factors: vertical electric field on the ground surface (Pulinets et al., 2000), variations of air conductivity (Pulinets and Davidenko, 2014), and vertical currents (Kuo et al., 2011). From the point of view of the experimental validation, the first one is closest to the truth. The values of the electric field measured in the ionosphere by in-situ probe from the satellite was within the range of the model calculations for the Alaska M8.2 earthquake 29 July 2021 (Hegai et al., 2023).

The question remains how to recognize that these temporal variations of TEC are really connected with earthquake preparation and are not something else? The answer is quite natural: the observed TEC variation should be local and should be somehow tied to the zone of earthquake preparation. Such an example is provided in Fig. 5. The positive TEC deviation over Greece on the series of differential GPS TEC maps looks like it is tied to the area where epicenter is marked by white cross: it is almost motionless during the whole day which is impossible for other types of the ionospheric variability which are usually driven by the local time.

We should underline that similar pre-earthquake variations are observed not only using the GPS TEC techniques but also by ground-based and topside vertical sounding of the ionosphere (Pulinets and Boyarchuk, 2004), as well as by in-situ satellite measurements (Chen et al., 2023). The only difference between all available technologies is that today GPS TEC data are the most accessible and operative source of ionospheric information.

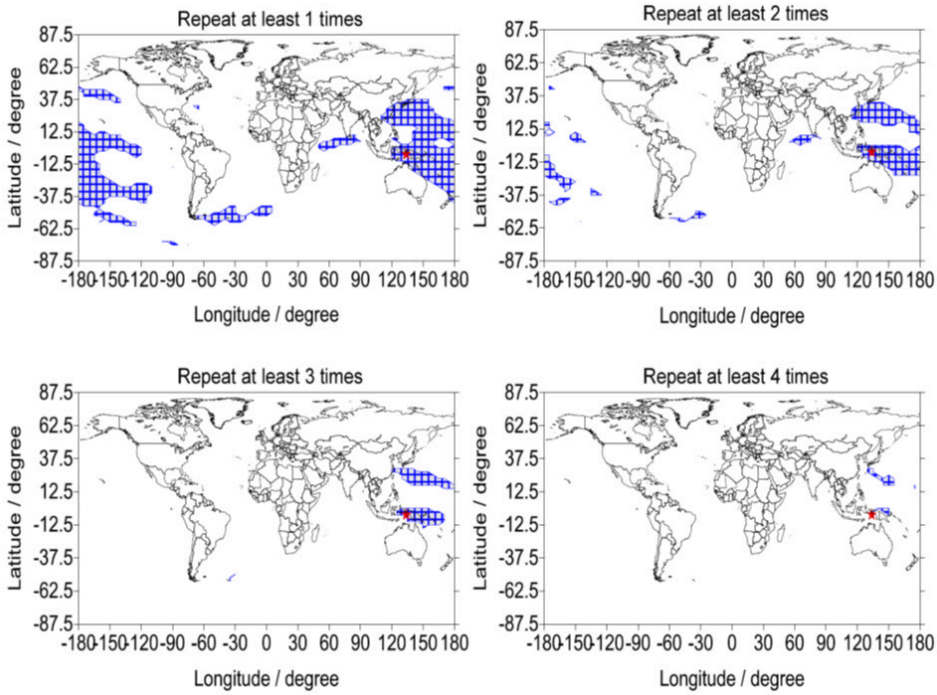


Figure 6 Locations of the 30-day extreme enhancement that repeatedly appeared at various time points on 28 September 2010 (Yao et al., 2012).

According to the position of the PEID, they have some peculiarities which were revealed by the satellite measurements: first by topside sounding (Pulinets and Boyarchuk, 2004) and then by the CPS TEC (Yao et al., 2012) and in-situ satellite measurements (Zhima et al., 2022). The PEID registered before an earthquake in the low latitude and middle/low latitude sometimes have reflection in the magnetically conjugated point which is clearly seen in Fig. 6 (Yao et al., 2012). The figures show the positive PEID as a maximum 30-day deviation according to the number of repetitions in the global TEC maps (from 1 to 4). At the fourth panel are seen the areas to the east from the epicenter of the M7 earthquake in Indonesia on 29 September 2010 and in the conjugated points in the Northern hemisphere which were registered one day before the main shock, i.e. 28 September. The effect of conjunction confirms the electric field penetration mechanism, which after penetration in the ionosphere is mapped to the conjugated hemisphere along the geomagnetic field lines which have practically infinite field-aligned conductivity.

Have the local ionospheric disturbances over the electrical disturbed areas in troposphere been observed in other cases except earthquake preparation zones? Yes, we have plenty of examples of natural phenomena such as hurricanes (Bondur and Pulinets, 2012), volcano eruptions and dust storms (Pulinets et al., 2022b). In Fig. 7 the remarkable positive variation of the peak electron concentration $NmF2$ (bold line) is registered over Katrina hurricane (Bondur and Pulinets, 2012). It is one more proof that PEID are the ordinary natural phenomena regularly registered in the ionosphere.

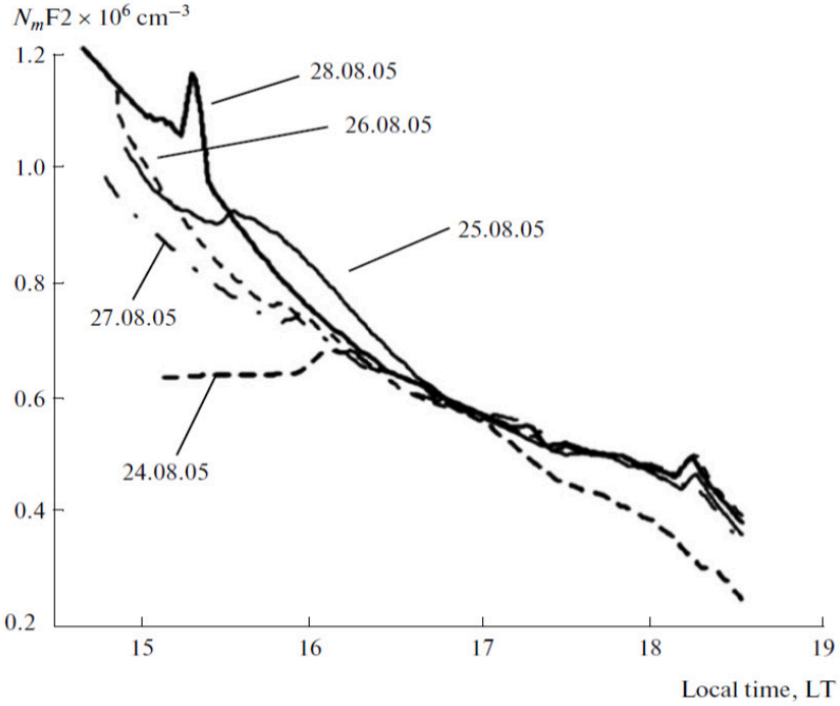


Figure 7 Variations in the electron concentration NmF2 over Hurricane Katrina according to data from GPS satellite no. 19 for the period from August 24 to 28, 2005.

Now we can generalize the main specific features of the pre-earthquake ionospheric disturbances:

1. PEID registered over the earthquake preparation zones are the result of atmospheric boundary layer local modification due near ground layer of atmosphere ionization by increased radon release from active tectonic faults
2. Intensity of PEID depends on the local time due to dynamics of atmospheric boundary layer
3. The sign of electron concentration deviation in the ionosphere depends on the column air conductivity and concentration of the large cluster ions with low mobility
4. For the low latitude PEID sometimes the conjugated effect is revealed

The information presented above describes only part of phenomena registered in atmosphere and ionosphere before the strong earthquake over the zone of earthquake preparation and mentioned in Fig. 1 because of the limit of the paper volume. Nevertheless, it provides major information on the physics of the generation of short-term precursors.

It is necessary to discuss one more question: why in the majority of publications on earthquake precursors do they have the label/earmark “anomalies” regardless of whether we were able to demonstrate that they are in the company of other natural phenomena which do not have this attribute.

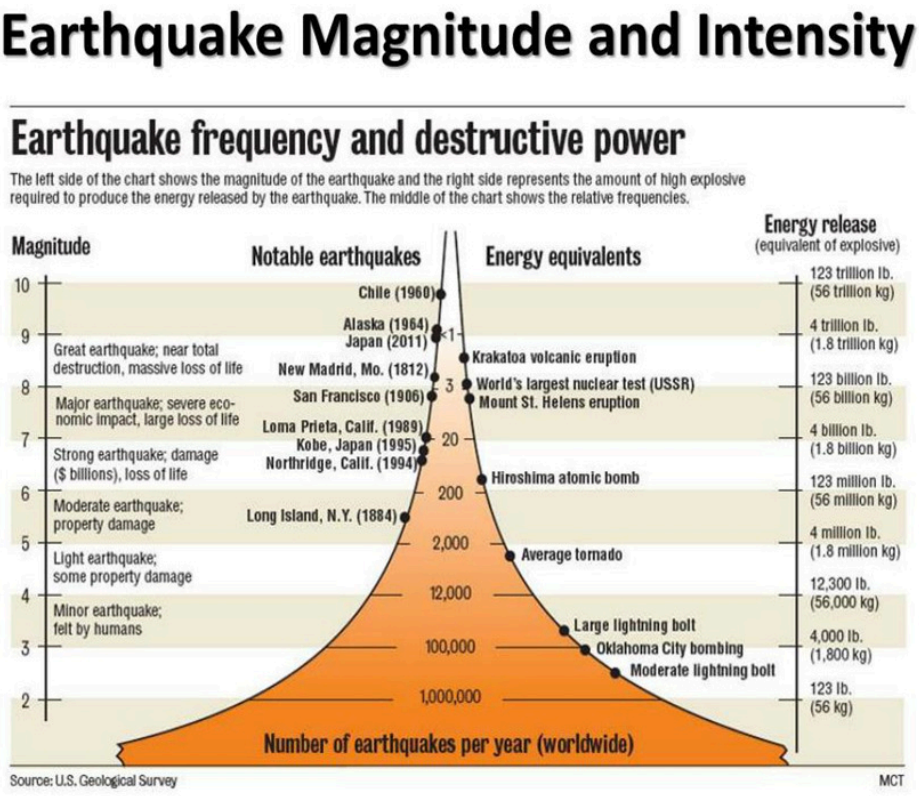


Figure 8 Magnitude, frequency and destructive power of earthquakes.

This is because of their low predictability. In the case of atmospheric thermal phenomena, the meteorologists do not know that a large amount of radon is released somewhere and they may expect a sharp drop of relative humidity and a rise of air temperature. This type of discrepancy between the meteorological forecast and the real atmospheric parameters is demonstrated in Fig. 11 of (Pulinets et al., 2023). The space weather experts considering the ionospheric phenomena are aware of the disturbances on the Sun and may expect some disturbances in the ionosphere two days after the solar flare, but the intensive disturbance in the ionosphere without any reason (if the possibility of pre-earthquake phenomena is not known) looks to them like an anomaly. We discuss the possibility of identification of the pre-earthquake phenomena in the next paragraph.

3 The problem of identification and predictability

Discussions on short-term earthquake prediction were mentioned in the Introduction and we will not return to this discussion. We will try to approach the problem from a common-sense perspective. In Fig. 8 the comparison of earthquakes having different

magnitudes with other disastrous phenomena of natural origin and nuclear explosion energies is shown.

Looking at Fig. 8 it is difficult to imagine that nothing happens over the ground surface before the release of such huge energies from the Earth's crust, so we will not discuss further the possibility of the absence of precursors. We deal with another problem: we do not know where or when a seismic shock will occur and how strong it will be. We see only one way to resolve this problem: continuous round the clock monitoring of the earthquake precursors, and only a specially created service can do this. No one country in the world has such a service, and this is the main reason for the absence of the short-term earthquake forecast – not scientists, not the lack of technologies, only good intentions and state resources are necessary. The next part will be devoted to the description of the technologies of the main parameters of the earthquake (place, time and magnitude) based on the precursor's features established by the LAIC physical model.

3.1 Detection of the epicenter position

The main feature used in the epicenter position is the precursor locality, and the fact that location of the precursor should be "tied" to the epicenter position. It was experimentally established that the maximum of precursor amplitude (regardless of whether it is a thermal or ionospheric precursor) not necessary coincides with the epicenter position. In this regard it is important to determine the position and size of the earthquake preparation zone (Dobrovolsky et al., 1979) depending on the earthquake magnitude:

$$R\ (\text{km}) = 10^{0.43M}, \tag{2}$$

where R is the radius of the earthquake preparation zone (EPZ) in kilometers, and M is the earthquake magnitude. Determining this zone, we know for sure that the earthquake epicenter should be inside this zone. Figure 9 demonstrates the properties of different precursors in relation to the EPZ. We used four different sources of the short-term precursors detection: a) differential GIM map registered 6 days before Kamchatka M7.2 earthquake on 30 January 2016 (Alekseev et al., 2021); b) ACP spatial distribution registered few weeks before the Kamchatka M7.2 earthquake on 30 January 2016; c) the series of OLR thermal spots registered before the Nepal M7.8 earthquakes on 25 April and 12 May 2015 (Ouzounov et al., 2016); d) distribution of electron concentration large deviations along the DEMETER satellite orbits before Chile M8.8 earthquake on 27 February 2010, and Chile M6.3 earthquake on 19 November 2007 (Li and Parrot, 2016).

Figure 9 needs more detailed comments regarding the procedures of the epicenter position determination. Figure 9a shows our attempts to determine the epicenter position using AI approach. Computer automatically detected the maximum of PEID which were 53° N and 159.7° E, this point is marked by the blue star. The real epicenter position was 54° N and 158.51° E and is marked by a yellow spot. The circles in the picture will be discussed in the section on magnitude estimation. Figure 9b shows that the ACP spatial distribution is not symmetrical in relation to the epicenter position and does not occupy all of the Dobrovolsky zone diameter. Here we have to apply the approach of multi-parameter monitoring where the ionospheric

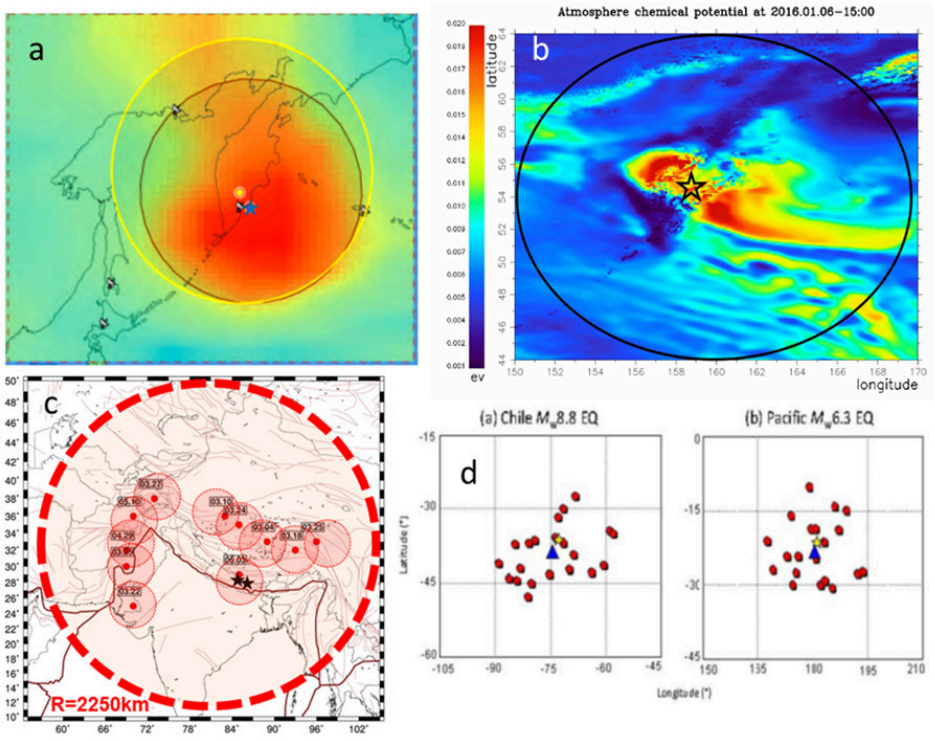


Figure 9 a) Differential GIM TEC map registered 4 days before the Kamchatka M6.9 earthquake on 3 March 2023. Epicenter position is marked by yellow spot, operator appointed epicenter position is marked by blue star; b) ACP spatial distribution for Kamchatka M7.2 earthquake registered a few weeks before the main shock on 30 January 2016, Dobrovolsky zone is marked by black oval; c) the series of positions of OLR thermal spots registered before the Nepal M7.8 earthquakes in 2015 (Ouzounov et al., 2021), Dobrovolsky zone is marked by red circle; d) distribution of electron concentration large deviations along the DEMETER satellite orbits before Chile M8.8 earthquake on 27 February 2010, and Chile M6.3 earthquake on 19 November 2007 (Li and Parrot, 2013).

map shown in Fig. 9a obtained for the same earthquake is a primary source for epicenter position determination, and ACP map is a proof that positive ionospheric disturbance is connected with earthquake, not with other sources of disturbances in the ionosphere.

Figure 9c demonstrates the dynamics of the process characteristic to the complex self-organizing systems (Knyazeva and Kurdiumov, 2003). Positions of OLR spots show the phase trajectory of strange attractor as the earthquake moment approaches. In this case we should consider the all complex of OLR spots positions to estimate the epicenter location.

Figure 9d demonstrates how the in-situ satellite measurements used for the epicenter position determination (Li and Parrot, 2013). For every case the coordinates of the maximal deviations of electron concentration measured by Langmuir probe are put in the map, and from the geometrically weighted distribution its weight center

determined (blue triangles). The position of the real epicenter is marked by the yellow spot.

It is obvious that we are dealing with a complex problem but with the fast developing of the AI technologies it seems that it will be successfully resolved.

3.2 Estimation of the time of earthquake

The 5 days lead time of ionospheric precursors arising before an earthquake was estimated as early as in 1998 (Pulinets, 1998). Different studies using the different technologies including the ground-based vertical sounding (Liu et al., 2004), GPS TEC (Liu et al., 2006), satellite measurements onboard the DEMETER satellite (Li and Parrot, 2013), satellite measurements onboard CSES1 satellite (Shen, 2023) give the numbers between 1 and 10 days, but the most probable value remains 5 days before the seismic shock. Of course, if we take into account the earthquake magnitude, the distance of the GPS receiver to the epicenter, or longitudinal distance of the satellite orbit to epicenter, the distributions of precursors become more complex and multidimensional (Le et al., 2011) but the order of magnitude for ionospheric precursors is clear, and from the perspective of the general approach it can be accepted as 5 days. As a kind of proof we provide the distributions obtained by the DEMETER and CSES1 Satellites during nearly 6 years of observations for each.

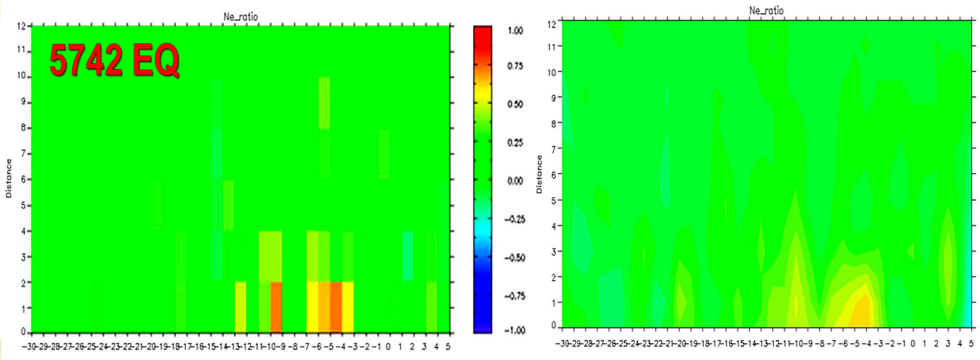


Figure 10 Left panel – leading time of ionospheric precursors distribution obtained by the Langmuir probe measurements onboard the DEMETER satellite for period 2004–2010; right panel – leading time of ionospheric precursors distribution obtained by the Langmuir probe measurements onboard the CSES1 satellite for period 2018–2023.

Thermal anomalies of different types have more complex dependencies. As we have seen in Fig. 9, the OLR anomalies may appear much earlier, approximately one month before the M7.8 Nepal earthquake on 25 April 2015, but again, on average, their lead time is also 5 days.

For ACP we provided the statistical studies for the Kamchatka earthquakes with M $\geq$ 6 during 10 years of observation (2005–2015) taking as a precursor two parameters: day of the monthly maximum of ACP in the earthquake epicenter, and day of sharp drop of ACP usually observed just before the main shock, or even on the day of earthquake. The distributions are shown in Fig. 11. It can be clearly seen that for

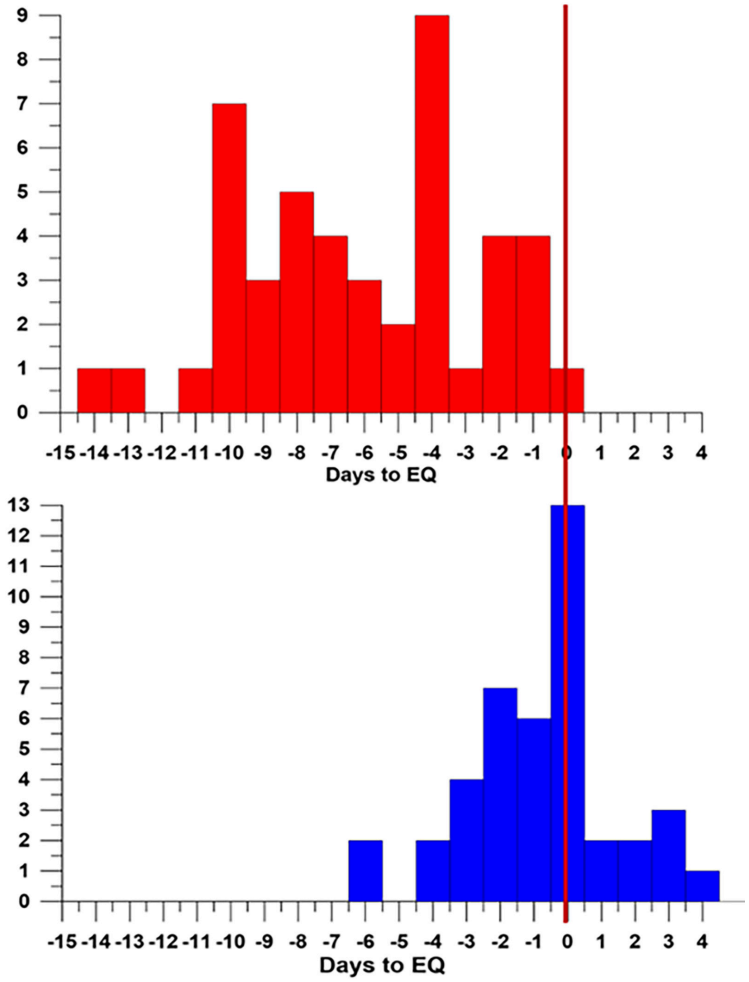


Figure 11 Top panel – distribution of the monthly maximum of ACP in relation to the day of earthquake marked as 0; lower panel – distribution of the ACP sharp drop in relation to the day of earthquake marked as 0.

the ACP maximum we observe two peaks: 10 days before and 4 days before. For ACP drop the peak is on the day of the earthquake.

3.3 Estimation of the earthquake magnitude

Here we should return to Fig. 9a where we tried to determine the earthquake magnitude automatically (Alekseev et al., 2021). The computer determined the Dobrovolsky zone which is presented as the dark colored circle, and according to (1) fives earthquake magnitude estimation as 7.07. The real Dobrovolsky zone for Zhupanovsky earthquake on 30.01.2016 has a radius of 1247 km which corresponds to magnitude 7.2.

From other distributions shown in Fig. 9 one understands that estimation of the

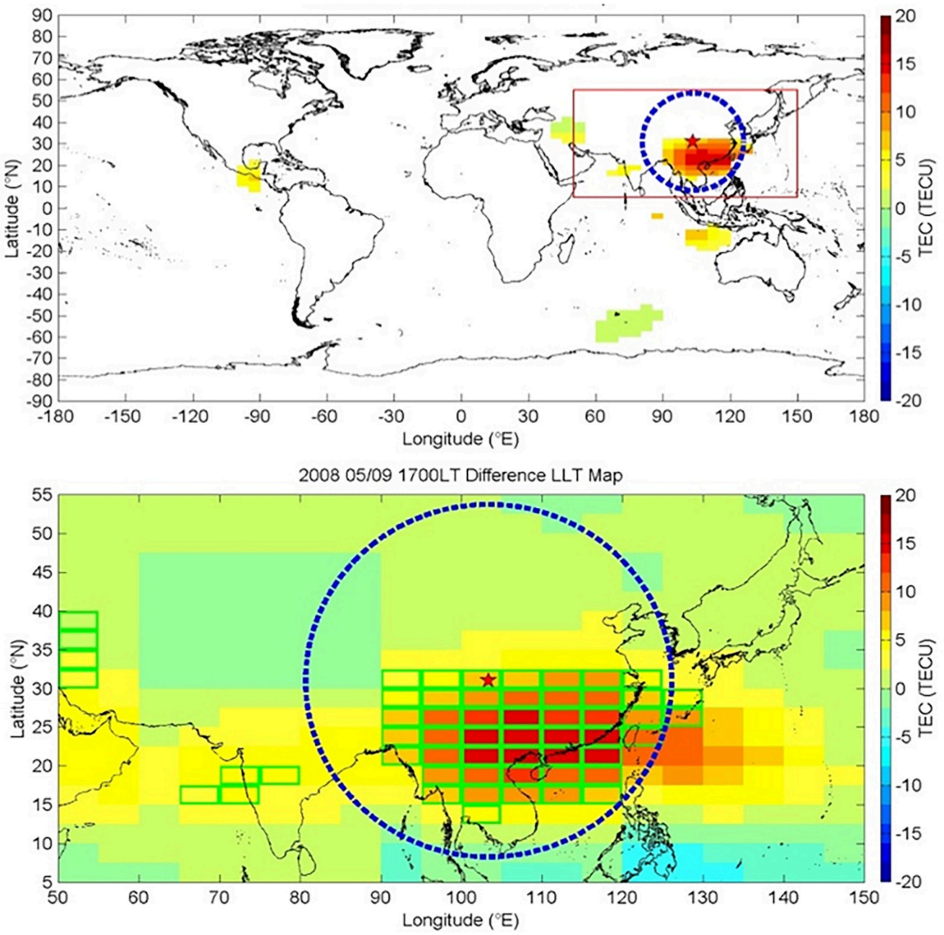


Figure 12 Top panel – global differential TEC LT map; bottom panel – regional differential LT map. Blue circles depict the Dobrovolsky zone. Red stars show the Wenchuan earthquake epicenter position.

earthquake magnitude is not a trivial task. The precursors do not fill the whole area of the Dobrovolsky zone which is consistent with its definition: the Dobrovolsky radius is the maximal distance at which the precursors MAY be observed, they should not obligatorily reach the edge of Dobrovolsky zone. Nevertheless, it is a good reference point for magnitude estimation. We recommend reading the reference publication (Liu et al., 2009) which describes the determination of PEID before the Wenchuan M8 earthquake 12 May 2008. To get the unambiguous answer about the size, position and dynamics of the ionospheric precursors for Wenchuan earthquake, we use the comparison of UT and LT global GIM TEC maps. We demonstrate only the small part of the whole procedure of determination the positive deviation of TEC 3 days before the earthquake in Fig. 12. The several features described earlier could be seen in the figure: the shift of the PEID in direction of geomagnetic equator, the conjugated effect on the global map and Dobrovolsky zone as indicator of the earthquake precursor.

3.4 The problem of the identification of precursors

During the many years of the studies of earthquake short-term precursory events, the opponents of the earthquake forecast claimed that precursors (even if they exist) are very weak and it is impossible to distinguish them from the effects of Space Weather in the ionosphere or high variability of atmosphere in case of the thermal precursors. We raised some questions with reference to this discussion in the text above, now let us summarize our arguments.

The first argument is the precursor's locality. From Fig. 9 we can conclude that the ionospheric and thermal effects are not connected with the Space Weather and atmospheric weather effects, and they are developed only within the zone of earthquake preparation contrary to the ionospheric effects of geomagnetic storms which have a global character. The most convincing proof of the precursor locality is demonstrated in the top panel of Fig. 12. We do not see any disturbances on the global map except for the one within the area of the Wenchuan earthquake preparation zone.

The second argument is the multiparameter approach, the example we see again in Fig. 9. We see both the ionospheric and thermal ACP precursors for the same Zhupanovsky earthquake at Kamchatka. It means that even one of the precursors is polluted by some strong disturbance of other origin, we have proof of earthquake preparation in the dynamics of precursor having other physical nature. Taking into account that we use more than two precursors for every earthquake, the probability for confusion with something else is very low. Again, we can recommend to read description of precursory period before L'Aquila earthquake in (Pulinets et al., 2012a).

The next argument is the strongest one and is connected with the physical nature of the precursors. The ionospheric precursors temporal behavior is strongly guided by the local time (Pulinets and Davidenko, 2014), especially by the atmospheric boundary layer behavior, which is not characteristic of other kinds of the ionosphere variability. In the case of the thermal/meteorological effects the difference of the bond

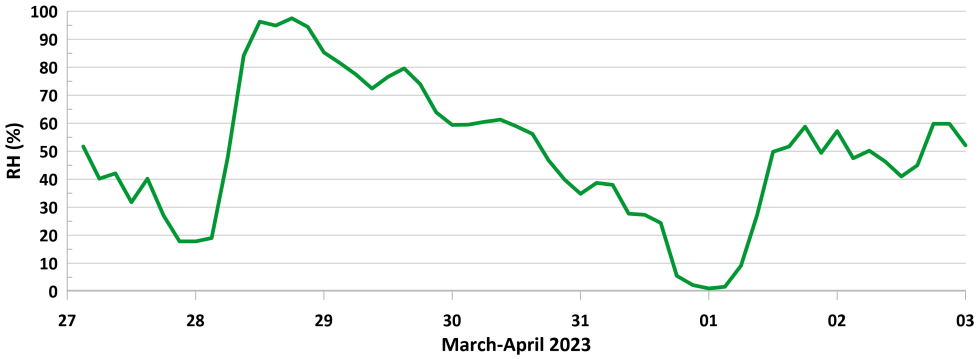


Figure 13 Air relative humidity variation near the Chilean coast around the time of M6.3 earthquake. The last argument is the temporal and spatial synchronization of precursors which demonstrate their concentration in space around the time of the main shock, in time with the approach of the main shock, and demonstrate propagation by altitude from the near ground disturbance to the upper atmosphere, ionosphere and even magnetosphere (Ouzounov et al., 2021; Pulinets et al., 2022a).

energy of water molecules in the ion cluster and the bond energy in pure water liquid may lead to the values of atmospheric parameters which are absolutely impossible to reach in natural conditions. Figure 13 shows the variation of the relative humidity in open ocean around the time of M6.3 earthquake near the Chilean coast which reaches a value near 2%.

4 Conclusions

We provided the main provisions of our LAIC model which give some fundamental understanding of basic physical processes that are responsible for generation of the short-term earthquake precursors in the atmosphere and ionosphere. It was difficult to go deeper in the physical problems underlying the complex system of Lithosphere–Atmosphere–Ionosphere coupling but we present a clear picture of how the system is organized.

We also tried to demonstrate how to reach the main goals of short-term forecasting of earthquakes. It is clear that the tasks are not simple, but again the direction in which the science and technology should move is quite clear. The progress is very strongly dependent on human and material resources. As long as the problem remains the property of a few individuals, it is difficult to expect much progress, especially as this progress will depend on organizing the teaching of subjects devoted to earthquake forecasting in institutes and universities. This is the main task for our future.

Acknowledgements

The work was carried out with the support of the Ministry of Science and Higher Education of the Russian Federation (theme “Monitoring”, state registration No. 122042500031-8).

References

Akhmamedov K. H. (1993) Geomagn. Aeron. 33, 135
Alekseev O. A., Pulinets S. A., Budnikov P. A. et al.(2021) Rocket Space Instr. Inf. Syst. 8, 3
Bondur V. G., Pulinets S. A. (2012) Izv. Atm. and Ocean Phys. 48, 871
Boyarchuk K. A. (1997) Izv. Atmos. Ocean. Phys. 33, 236 Boyarchuk K. A., Lomonosov A. M., Pulinets S. A. (1997), BRAS Phys./Suppl. Phys. Vibr. 61, 175
Chen W.; Marchetti D. Zhu K. et al. (2023) Atmosphere 14, 1527
Dobrovolsky I. P., Zubkov S. I., Myachkin V. I. (1979) PAGEOPH. 117, 1025
Geller R. J., Jackson D. D., Kagan Y. Y., Mulargia F. (1997) Science 275, 1616
Golubenko K., Rozanov E., Mironova I., Karagodin A., Usoskin I. (2020) Geoph. Res. Let. 47, e2020GL088619
Hegai V., Zeren Z., Pulinets S. (2023) Atmosphere. 14, 819

Holzer R. F. (1972) JGR 77, 5845
Hoppel W. A., Anderson R. V., Willett J. C. (1986) In: The Eart's Electrical Environment. National Academy Press, Washington. D.C. pp. 149–165
Knyazeva E. N., Kurdiumov S. P. (2003) in: The Problems of XXI Century Geophysics. Nauka Publ., Moscow, pp. 37–65 (in Russian)
Kuo C. L., Huba J. D., Joyce G., Lee L. C. (2011), J. Geophys. Res., 116, A10317
Larkina V. I., Migulin V. V., Nalivaiko A. V., Gershenzon N. I., Gokhberg M. B., Liperovsky V. A., Shalimov S. L. (1983) Geomagn. Aeronom. 23, 684
Le H., Liu J.-Y., Liu L. (2011) JGR. 116, A02303
Li M., Parrot M. (2013) JGR. 118, 3731
Liu J.-Y., Chen Y.-I., Jhuang H.-K., Lin Y.-H. (2004) TAO. 15, 371
Liu J.-Y., Chen Y.-I., Chuo Y. J., Chen C. S. (2006) JGR. 111, A05304
Liu J.-Y., Chen Y.-I., Liu C.-H. (2009) JGR. 114, A04320
Main I. (1996) Rev. Geophys. 34, 433
Mareev E. A. (2010) Phys.-Uspekhi 53, 527
Mil'kis M. R. (1986) Izv. Earth Phys. 22, 195
Mironova, I.A., Aplin, K.L., Arnold, F. et al. (2015) Space Sci Rev. 194, 1
Morozova L. I., Nikolaev A. V., Pulinets S. A. (2020) Geol. Geophys. Rus. South. 10, 58
Mühleisen R. (1977) In: Electrical Processes in Atmospheres. H. Dolezalek and R. Reiter eds. Dr. Dietrich Steinkopff, Darmstadt. pp. 467–476
Nikiforova N. N., Michnowski S. (1995) IUGG XXI General Assembly Book of Abstracts, Boulder, CO. VA11D-16
Ouzounov D., Bryant N., Logan T., Pulinets S., Taylor P. (2006) Phys. Chem. of the Earth. 31, 154
Ouzounov D., Pulinets S., Davidenko D. et al. (2016) Geophys. Res. Abstr. 18, EGU2016-3496
Ouzounov D., Pulinets S., Davidenko D. et al. (2021) Front. Earth Sci. 9, 757358
Pulinets S. A. (1998) Adv. Space Res. 22, 903
Pulinets S.A. (2009) Adv. Space Res. 44, 767
Pulinets S. A., Khegai V. V., Boyarchuk K. A., Lomonosov A. M. (1998) Phys.-Uspekhi 41, 515
Pulinets S. A., Boyarchuk K. A., Khegai V. V., Kim V. P., Lomonosov A. M. (2000) Adv. Space Res. 26, 1209
Pulinets S. A., Legen'ka A. D., Gaivoronskaya T. V., Depuev V. K. (2003) J. Atm. Solar Terr. Phys. 65, 1337
Pulinets S. A., Boyarchuk K. A. (2004) Ionospheric precursors of earthquakes. Springer, 312 pp.
Pulinets S., Davidenko D. (2014) Adv. Space Res. 53, 709
Pulinets S., Ouzounov D. (2018) The possibility of earthquake forecasting. Learning from Nature, IOP Publishing, Bristol, 167 pp.
Pulinets S., Ouzounov D., Karelin A., Boyarchuk K. (2022a) Earthquake Precursors in the Atmosphere and Ionosphere. New Concepts. Springer Nature. 312 pp.
Pulinets S.A., Davidenko D.V., Pulinets M.S. (2022b) Adv. Space Res., 69, 4319
Pulinets S., Budnikov P., Karelin A., Žalohar J. (2023) JASTP 246, 106050
Scholz C. H., Sykes L. R., Aggarwal Y.P. (1973) Science 181, 803

Shen X. (2023) IMCP International Workshop, September 14–17, NSSC-Huairou Campus, Beijing

Tacza, J., Raulin, J.-P., Mendonca (2018) JGR Atmospheres. 123, 11,970

Timofeev V. E., Grigor'ev V. G., Morozova E. I. et al. (2003) Geomagn. Aeron. 63, 636

Vershinin E. F., Buzevich A. V., Yumoto K. et al. (1999) in "Atmospheric and Ionospheric Electromagnetic Phenomena Associated with Earthquakes", Ed. by M. Hayakawa. Terra Scientific Publishing Company, Tokyo. 513

Zhima Z., Yan R., Lin J. et al. (2022) Remote Sens. 14, 905